Pergamon

Journal of Structural Geology, Vol. 17, No. 4, pp. 509 to 517, 1995

0191-8141/95 $9.50 + 0.00

0191-8141(94)00080-8

Asymmetric shape preferred orientations as shear-sense indicators

DAVID SHELLEY

Department of Geology, University of Canterbury, Christchurch, New Zealand

(*Received* 4 *January* 1994; *accepted in revised form* 21 *June* 1994)

Abstract—Mineral shape preferred orientations can be characterized by plotting aspect ratios against grain-length orientation, and such plots commonly display asymmetric patterns in *XZ*-sections (perpendicular to foliation and parallel to the direction of maximum elongation). In most cases, the asymmetries cannot be discerned by superficial examination of thin sections. The sense of asymmetry can be defined by: (a), the shape of the highest aspect-ratio per grain-length orientation curve, and (b), the relative orientations of the most elongate grain and the mean or median of the population as a whole. Observed senses of asymmetry display consistent relationships to known senses of shear, and they therefore provide a useful alternative to, or check on, other methods of shear-sense determination. Examples of quartz, plagioclase, microcline, amphibole and biotite shape preferred orientations are described, and they include recrystallized mosaics as well as populations of discrete mineral grains. The examples include mineral preferred orientations that evolved by plastic deformation, anisotropic crystal growth, and mechanical rotation of inequidimensional grains.

INTRODUCTION

Most of the literature on mineral preferred orientations is concerned with lattice preferred orientations (LPOs). The subject of shape preferred orientations (SPO's), especially in metamorphic rocks, has been relatively neglected, despite the fact that foliations and mineral lineations are defined fundamentally by SPO's. Although there is an extensive literature on the theoretical and experimental behaviour of rigid particles of different shapes during Newtonian simple shear flow (e.g. Ildefonse *et al.* 1992, and references therein), there has been little analysis of the SPO's to be expected during the processes of plastic deformation or competitive anisotropic growth. Only a few papers describe in detail the real SPO's of metamorphic rocks (e.g. Ildefonse *et al.* 1990, Miyake 1993, Shelley 1979, 1989a), and most petrologists have been content to define the orientation of these structures in terms of a simple plane and direction, judged roughly in hand-specimen. The reality is that mineral grains constituting a foliation or lineation have diverse ranges of shape orientation and aspect ratio, as displayed in Fig. 1.

Such diagrams often disclose skewed data, and the purpose of this paper is to document and discuss such asymmetries, and to explore the possibility that the asymmetries are related in some consistent way to senses of shear during SPO development.

Mineral preferred orientations can be classified according to the mechanism of formation as either *P*-types, due to plastic deformation, *G*-types, due to competitive anisotropic growth (or its complement, solution), or *M*-types, due to mechanical rotation of inequidimensional grains (Shelley 1989b). This terminology is used throughout the paper.

MEASUREMENT METHODS

All the data in this paper derive from the measurement of grain sizes, aspect ratios, and grain-length orientations using a polarizing microscope. In all cases,

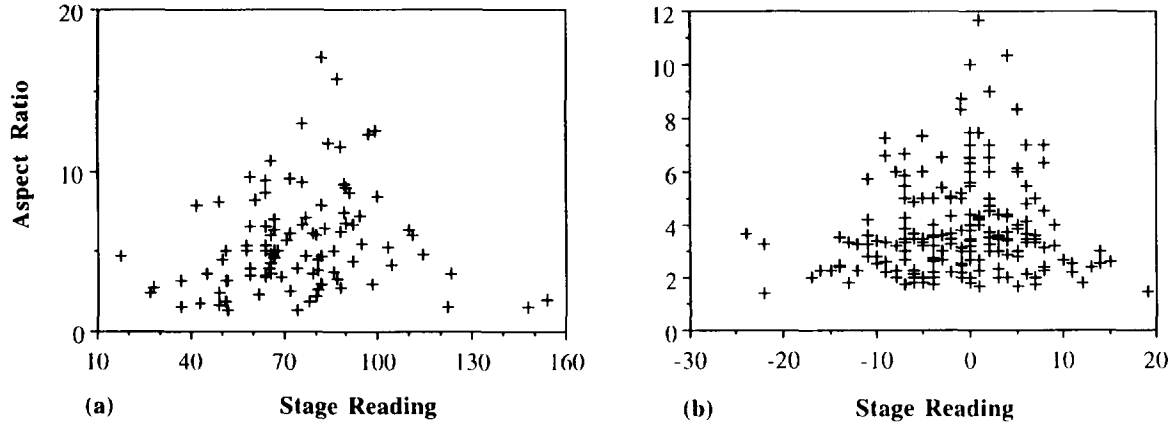

Fig. 1. Scatter plots of grain aspect ratios (length/width) against grain-length orientations (given by stage readings). (a) One hundred measurements for biotite in KP3, a deformed granite, Fiordland, New Zealand. (b) Two hundred measurements for albite in DS970, a quartzofeldspathic schist from the Haast Schists, New Zealand. Discussion in text.

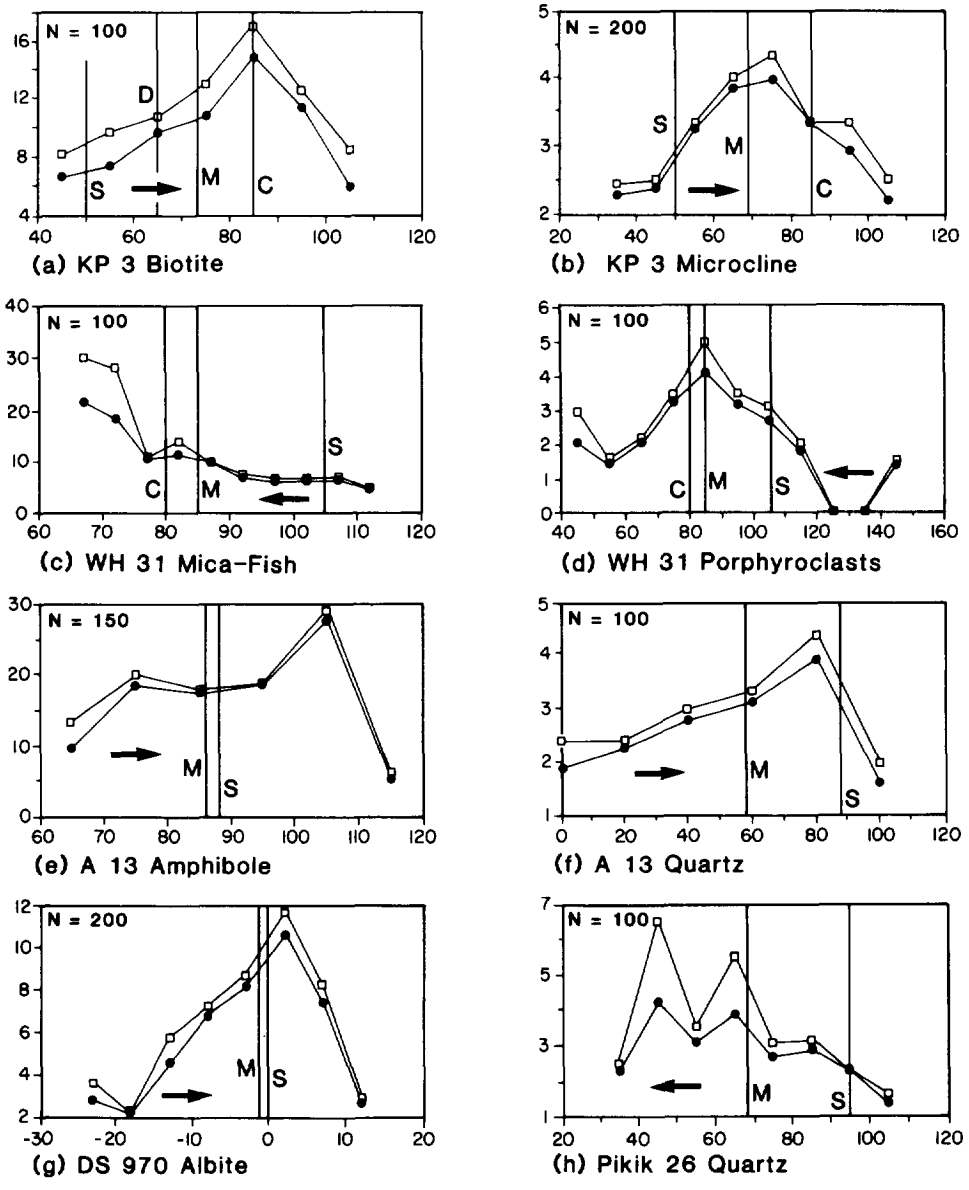

Fig. 2. Curves for a variety of specimens and minerals, derived from data in scatter plots such as Fig. 1. The horizontal axes record the stage readings for grain-length orientations and the vertical axes record aspect ratios (length/width). Upper curves represent the highest aspect ratios, the lower curves the mean aspect ratios of the three most elongate grains, for particular grain-length orientation categories. Various other orientations are marked: M = mean and median of the grain-length orientations. D = mode of grain-length frequencies. S = S-planes in S–C mylonitic structures in (a)–(d), macroscopic metamorphic layering in (c)–(g), and the orientation of elongate quartzite fragments in (h). C = C-planes in S–C mylonitic structure in (a)–(d). The arrows indicate the sense of rotation, as judged from other criteria. N = number of measurements. Discussion in text.

the XZ-section perpendicular to foliation and parallel to a mineral lineation or elongation direction was chosen for measurement. As noted in Shelley (1989a, 1992), one method of characterizing shape preferred orientations is to use a scatter plot (Fig. 1) of aspect ratio (length/width) against grain-length orientation (given by a stage reading).

Asymmetries are often immediately evident (e.g. Fig. 1a), but a better way to display skewness in the data is to plot the highest aspect ratio curves for particular grain-length orientation categories together with the grain-length orientation mean and median (Figs. 2a & g, for example, are derived from Figs. 1a & b). In order to guard against the possibility of the odd grossly aberrant datum distorting the highest aspect ratio curves, curves for the mean of the three highest aspect ratio grains in any one orientation category are also plotted. The size of grain-length orientation categories is chosen so that a reasonably smooth distribution of data is displayed. One hundred or more measurements are made for each specimen, and I have found that orientation intervals of 5° or 10° usually produce smooth curves. Outliers of data in grain-length orientation categories of low frequency (less than or equal to 2% of the data) often severely distort the highest aspect ratio curves, and have been eliminated.

A simple test of the validity of data (as with LPO diagrams) is reproducibility, and by the time 100 (some-

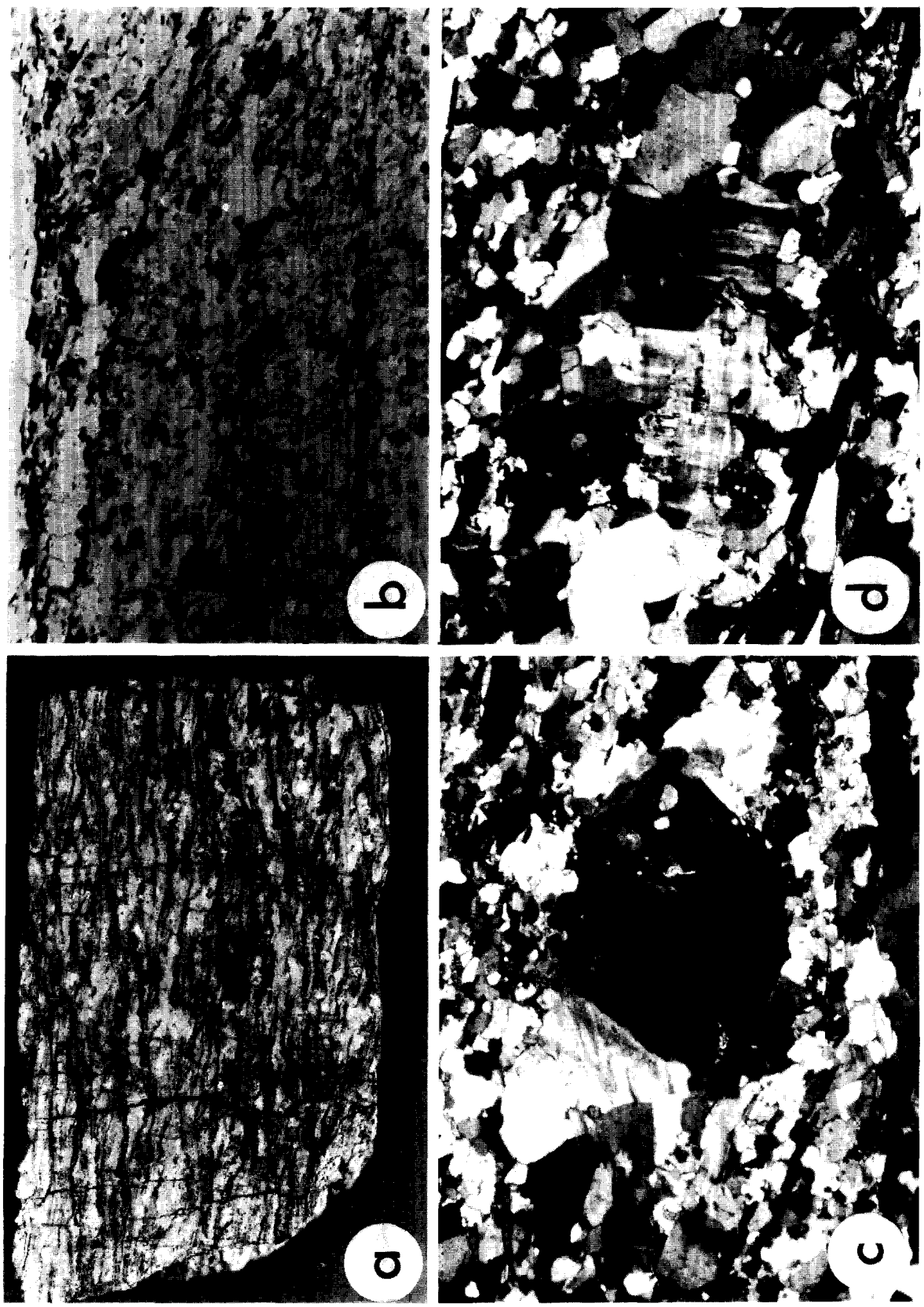

Fig. 3. Specimen KP3. a deformed granite from Fiordland. (a) Surface cut parallel to lineation and perpendicular to foliation illustrates the mylonitic aspect and a sinistral shear sense (anastomosing *S–C* planes and σ-type porphyroclast systems). Surface measures 87 × 52 mm. (b) Thin section view (between parallel polarizers) to illustrate metamorphic biotites that define the *S–C* planes. View measures 8.6 × 5.8 mm. (c) & (d) Microcline porphyroclasts (in crossed-polarized light) with coarse recrystallized microcline tails that step up to the left. In (c) a quartz ribbon parallel to *C*-planes runs east–west at the bottom of the view, and in (d) a *C*-plane defined by biotite runs subparallel to the base of the photo. The porphyroclasts and their tails define typical σ-type shapes relative to the *C*-planes. (c) & (d) views measure 2.82 × 2.11 mm.

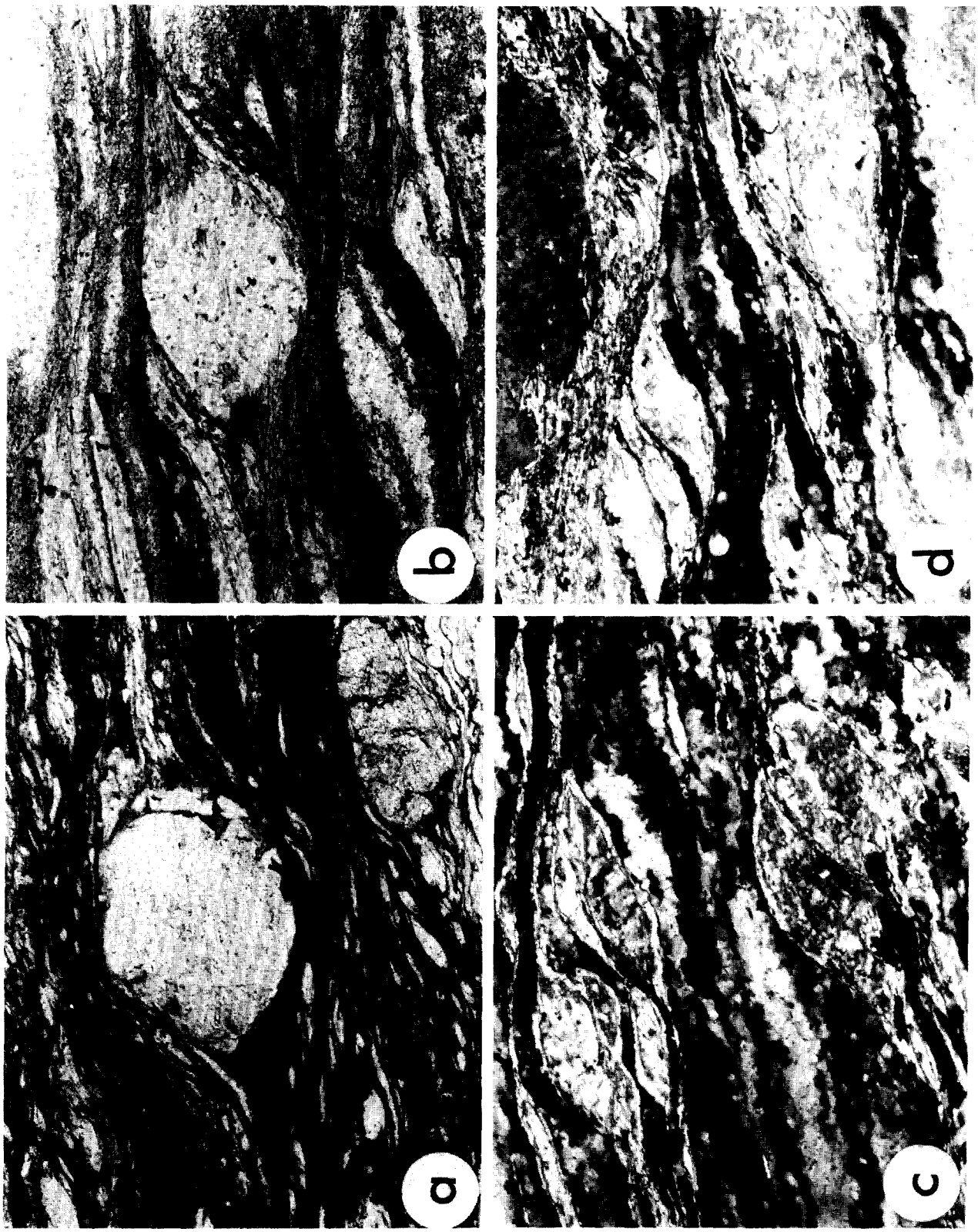

Fig. 4. Specimen WH31, a granitoid mylonite from the Charleston Metamorphic Complex. A dextral sense of shear is indicated in (a) by a σ-type feldspar porphyroclast system, in (b) by a σ-type mica porphyroclast system and mica-fish, and in (c) & (d) by mica-fish. (a) & (b) are in plane polarized light, (c) & (d) in crossed-polarized light. Views measure 2.8×2.2 mm (a), 0.64×0.5 mm (b), and 0.74×0.58 mm (c) & (d).

times 150 or 200) data are plotted, the essential characters of the curves and sense of skew have been found not to change.

An often frustrating aspect of this work is measuring the length, width, and orientation of irregularly shaped grains. The length is usually easily defined, but for curved, rhomboidal, and irregularly-shaped grains, determination of width and a precise grain-length orientation can be difficult. With regard to measuring grain-length orientations, I recommend grains be positioned north–south rather than east–west (there is a tendency to place grains that are east–west in a position of 'easy repose' which may differ by several degrees from the most symmetrical position). In the north–south position, the most suitable grain-length orientation can usually be determined confidently by trial rotations either side of a 'possible' position. With regard to widths, I have consistently measured the dimension perpendicular to length that combined with the length can form a simple rectangle that encompasses the entire grain (rather than some mean width, or the uniform width of irregular and curved grains). Nevertheless, there are always some grains that defy measurement. In particular, grains of very low aspect ratio often have to be disregarded, and the low aspect ratio regions of scatter plots must therefore be regarded with special care.

DESCRIPTIONS OF THE ASYMMETRIC SPO's

Five specimens, described in turn below, are used to illustrate asymmetric SPO's. It should be noted that asymmetries revealed are usually not obvious in thin section, and would not normally be observed during routine petrography. The only exception is for the mica-fish in specimen WH31.

In all the SPO diagrams (Fig. 2), the arrow shows the sense of shear that was predetermined using other criteria such as mica-fish, quartz *c*-axes girdles, etc. In Fig. 2(a), for example, the sense of shear is such that it would cause grains with grain-lengths at 60° (stage reading) to rotate towards a new orientation with lengths oriented at say 80°.

KP3—deformed granite from Fiordland, New Zealand

KP3 displays shear-sense indicators typical of a granite–mylonite (Berthé *et al.* 1979, Passchier & Simpson 1986), namely σ-porphyroclast systems (involving relics of microcline with coarse, dynamically recrystallized tails), and *S–C* planes defined mainly by biotite (Fig. 3). There is, however, a high degree of recrystallization and crystallization, and the rock is more appropriately termed an orthogneiss than a granite–mylonite.

The biotite (Fig. 3b) is not in the form of mica-fish or porphyroclasts, but is fine-grained, generally undeformed, and the product of a subsolidus neocrystallization (median of 100 grain-lengths is 0.17 mm). The biotite SPO diagram (Fig. 2a) shows a distinct asymmetry so that the orientation of the highest aspect ratio grains (85°) is displaced from the centre of the total range of grain-length orientations (40–110°). The mean, median and modal orientations for the total set of data are 74.41°, 72° and 65°, respectively.

Microcline occurs in elongate ribbon-like domains consisting of dynamically recrystallized mosaics (median of 200 grain-lengths is 0.25 mm). Some of these domains are tails to the microcline σ-porphyroclast systems (Figs. 3c & d). The SPO diagram for the recrystallized grains (Fig. 2b) shows a weak asymmetry, but again the highest aspect ratios (at 75°) are displaced relative to the mean and median orientations (69.73 and 68°) in the same sense as in the biotite SPO diagram.

WH31—granitoid–mylonite, Charleston Metamorphic Complex, New Zealand

This mylonite contains excellent examples of the widely accepted shear-sense indicators, mica-fish, *S–C* planes and σ-porphyroclast systems (Fig. 4). The mica-fish diagram (Fig. 2c) illustrates an extreme degree of asymmetry with very thin plates of high aspect ratio along planes of shear, and relatively thick grains (the mica-fish themselves) occupying positions closer to the *S*-planes.

The feldspar porphyroclast SPO diagram exhibits a weak asymmetry (Fig. 2d). The shapes of the curves have the same sense of asymmetry as the mica-fish curves, but the mean and median orientations and the orientation of the highest aspect ratio grains coincide.

A13—blueschist-facies metachert, Franciscan, California

This rock is fully described in Shelley (1994). It has a very strong lineation defined by alkali-amphibole, which according to the evidence of 'spider-texture' was formed rather like slickenfibres along shear-planes. The dynamically-recrystallized quartz displays *en masse* a grain-shape foliation at a moderate angle to the amphibole lineation and oblique to a quartz *c*-axes crossed girdle (Shelley 1994, figs. 4b and 3a). The spider texture and the obliquity between quartz grain-shape and *c*-axes girdles provide indications of shear-sense.

The amphibole SPO diagram (Fig. 2e) shows a peak aspect ratio at 105°, quite different from the mean and median grain-length orientations at 86.73° and 86°. The quartz diagram (Fig. 2f) shows a peak aspect ratio at 80°, and mean-median orientations at 57–58°. It is important to note that neither of these orientations coincide with the orientation of the grain-shape foliation which can be judged *en masse* in thin section (Shelley 1994, fig. 4b) to be at 48° (an orientation frequency curve for the A13 quartz data—not given here—does, however, display a strong peak at this orientation).

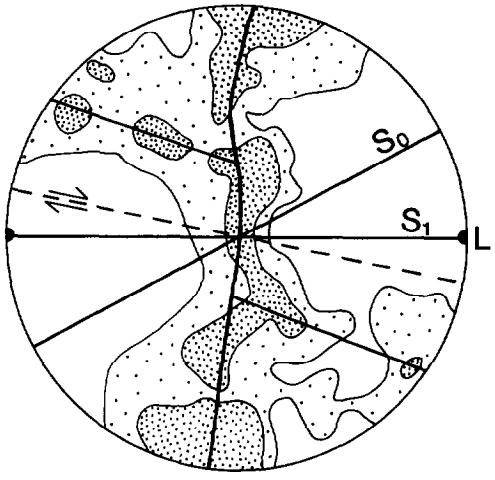

Fig. 5. Composite contoured equal area projection of 2400 quartz *c*-axes measured in several specimens of quartzite from Takaka Hill, Nelson, New Zealand. The skeleton of the pattern provides the sense of shear indicated. S_0, S_1 and L = bedding, foliation and lineation. Contours at 1 and 1.4% (max. 2.4%) per 1% area.

DS970—greenschist facies quartz–albite–mica schist, Otago, New Zealand

The rock is described fully in Shelley (1989a). A sense of shear is indicated by the quartz *c*-axes girdle oblique to foliation (Shelley 1989a, fig. 12a). Albite occurs as discrete, sometimes euhedral grains within mosaics of similar sized quartz, or embedded in micas, and its SPO pattern (Figs. 1b and 2g) has an obvious asymmetry.

Pikik26—quartzite, Pikikiruna Schist, New Zealand

Pikik26 is from the lower limb of a great recumbent fold affecting rocks of the Takaka Terrane in northwest Nelson (Shelley 1981), and consists almost entirely of a mosaic of dynamically recrystallized quartz grains. The common skeletal pattern of *c*-axes for several specimens of this quartzite, shown to be a useful method of kinematic analysis by Lister & Williams (1979), Behrmann & Platt (1982) and Vissers (1993), is given here in the form of a composite quartz *c*-axes diagram (Fig. 5). This kind of asymmetric type-1 crossed-girdle pattern of quartz *c*-axes is very similar to that used by Lister & Williams (1979) and Behrmann & Platt (1982) as a shear-sense indicator, and for the Pikikiruna Schist indicates a sense of shear from the western quarter. The SPO diagram (Fig. 2h) again displays the characteristic asymmetries and relationships found in the previous examples.

RELATIONSHIPS BETWEEN ASYMMETRIC SPO's AND THE SENSE OF SHEAR

In all of the examples above and shown in Fig. 2, there is a consistent relationship between predetermined senses of shear and the asymmetric SPO's. It can be described as follows:

(a) The sense of rotation is such that grains with length orientations represented by the flatter (longer) part of the aspect-ratio curves would rotate towards the orientation of the most elongate grain.

(b) The sense of rotation is also from the mean or median grain-length orientation towards the orientation of the most elongate grain.

The only exception to these rules is found in Fig. 2(d) where the mean and median of the grain-length orientations coincide with the peak aspect ratio orientation.

To understand why these relationships exist, it is necessary to consider separately the development of SPO's according to the three possible mechanisms of formation.

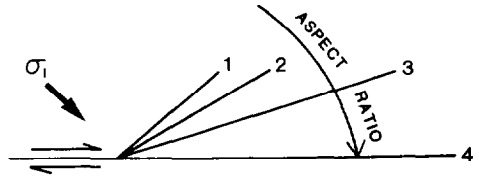

Fig. 6. Diagram to show the relationship between the maximum principal compressive stress (σ_1), the sense of shear on the plane of maximum shearing stress, and four grain-length orientations and aspect ratios, as discussed in the text.

MECHANISMS OF PREFERRED ORIENTATION DEVELOPMENT

P-*type SPO development*

A perfectly homogeneous plastic deformation of a regular crystal mosaic undergoing simple shear will produce a perfectly uniform array of grains with identical aspect ratios and orientations. However, it is commonly the case that (a), the deformation on the grain scale is heterogeneous, and/or (b), dynamic recrystallization takes place and/or (c), there is a strain partitioning similar to that responsible for *C–S* plane development in mylonites. In all such cases, an asymmetric SPO will develop so that the most elongate grains have an orientation closest to the plane of maximum shear-stress (Fig. 6).

Consider, for example, the case of (b) above. Dynamic recrystallization tends to change elongate deformed grains to equidimensional shapes. Grains that survive this process will become increasingly elongate as they rotate into orientation (3) of Fig. 6, whereas well-crystallized grains will only record the last increment of strain in orientation (1). Grains of intermediate aspect ratio will have orientations like position (2). Aspect ratios increase from orientations (1) to (3), the mean orientation lies somewhere between (1) and (3), and the shear sense is given by rotating grains of orientation (1) into orientation (3). Such a process of SPO development probably applies to the examples of microcline and quartz in Figs. 2(b), (f) & (h), all of which result from dynamic recrystallization.

These relationships would be exaggerated in the case of strain partitioning (*S–C* mylonites, for example), where unrecrystallized quartz grains caught up in zones

of severe strain (the *C*-planes) are very much more elongate (orientations 3–4) than grains recording slighter strains parallel to *S* (orientations 1–2). The shear-sense is again the same as if grains of orientation (1) are rotated into orientations (3) or (4).

G-type SPO development

Competitive anisotropic growth (or solution) is a potent mechanism for producing preferred orientations (Cox & Etheridge 1983, 1989, Shelley 1989a, 1994, Hippertt 1994), and given the essential fact that metamorphic minerals nucleate and grow during deformation, it is probably more common than is recorded in the literature. Competitive anisotropic growth may vary from the small late increments in grains of orientation (1) (Fig. 6) through to the possibly very large strains recorded by slickenfibre-type grain growth at steps on shear-planes (orientation 4 in Fig. 6). As with *P*-type SPO developments, the shear-sense is as if grains of orientation (1) had been rotated into orientations (3) or (4). The probable mechanism for the development of amphibole fabrics in A13 and albite fabrics in DS970 is competitive anisotropic growth (Shelley 1989a, 1994) which is therefore the probable explanation for the relationships in Figs. 2(e) & (g). With regard to the biotite in KP3 (Fig. 2a), the literature on sheet-silicate preferred orientations shows that both *M*-type and *G*-type processes are commonly advocated. Despite the mylonitic aspect of this deformed granite, the biotite texture is clearly that of newly crystallized and generally discrete fine grains set amongst a mosaic of dynamically recrystallized feldspar and quartz. A *G*-type mechanism seems more likely than an *M*-type, as explained below.

M-*type SPO development*

A variety of potential *M*-type mechanisms for producing mineral preferred orientations exists: (1) The March (1932) model assumes a homogeneous deformation in which platy or prismatic crystals behave in an identical manner to the matrix (and behave therefore as passive markers). Despite the apparent lack of realism in this model, it nevertheless predicts reasonably well the strength of sheet-silicate preferred orientations in slates (Oertel 1985a & b). (2) The tumbling behaviour of rigid crystals during laminar flow of a viscous fluid has been discussed in relation to igneous fabrics by several workers (e.g. Fernandez *et al.* 1983, Shelley 1985, Fernandez 1987, Benn & Allard 1989, Higgins 1991), and the same concept for simple shear deformation of metamorphic rocks has been discussed by Ildefonse *et al.* (1990), for example, in relation to glaucophane schists. (3) In rocks undergoing a volume reduction, either by loss of water or by solution transfer (removal of silica from sheet-silicate-rich layers), the sheet-silicates may rotate into parallelism simply by removal of the intervening material. (4) In mylonites, the cataclastic flow of mica tends to smear cleavage fragments out along shear planes. This is a process involving mechanical rotation of existing material, but material that cannot be considered rigid. Geometrically, the process is akin to gliding on {001}, and in that respect is similar to *P*-type mechanisms.

The strict applicability of *M*-type mechanisms to metamorphic fabrics is a very moot point. Tullis (1976), for example, points out that much the same fabric may develop regardless as to whether or not the crystals are growing or recrystallizing during strain, and in many examples of supposed *M*-type fabrics it is clear that the crystals did not simply exist as discrete pre-existing crystals, free to rotate in a ductile matrix, but that they crystallized during metamorphism, often forming an interlocking array of subhedral grains that in their present state could not possibly have undergone an *M*-type process.

The example of the biotite in KP3 (Fig. 2a) is a good example of the difficulty of advocating an *M*-type mechanism. The March model, for example, describes a homogeneous deformation in which the elongate crystals merely act as passive markers. This is incompatible with the observation of the asymmetric preferred orientation in which the mode and mean orientations are different from that of the most elongate crystals. Model 2 is inappropriate because the biotite cannot be regarded as relatively rigid material amongst the mosaics of feldspar and quartz. There is no evidence for concentration of the biotite as a result of removal of intervening material by solution transfer (model 3), and the biotite forms newly crystallized grains, not the shredded material of mica-fish porphyroclasts (model 4).

It is difficult, in my opinion, to select a wide range of unequivocal examples of *M*-type fabrics. The two examples I did select involve porphyroclasts in a mylonite, namely the mica-fish and σ-type feldspar-porphyroclasts of WH31. In Figs. 2(c) & (d), the '*C*' plane indicated is what most observers would call the *C*-plane of an *S*–*C* mylonite. The SPO analysis of mica-fish suggests, however, that the actual planes of maximum shearing stress, along which very elongate cleavage slices have been smeared, are oriented at stage reading 65°. The '*C*'-plane at 80° represents a mylonitic foliation related to the strain of quartz ribbons. The diagram shows that mica-fish have been rotated so that their lengths lie almost entirely between the '*S*'-plane and the plane of shearing at 65°.

The feldspar porphyroclasts of WH31 are certainly examples of rigid bodies in a ductile matrix, in which case the *M*-type model 2 (above) needs to be considered. This model has been applied in most detail, as far as SPO's are concerned, to igneous rocks (Blanchard *et al.* 1979, Fernandez *et al.* 1983, Shelley 1985, Fernandez 1987, Benn & Allard 1989, Higgins 1991). The most detailed SPO analysis is that of Benn & Allard (1989), and they document the typical imbrication where the most elongate grains are oriented at a small angle to the plane of laminar-flow, a semi-stable position that is enhanced by any 'tiling' or interaction of the crystals undergoing rotation. If the shear strain exceeds 5, the long axes of the most elongate grains will rotate past the

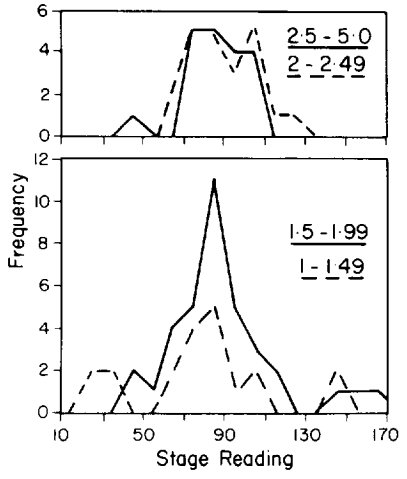

Fig. 7. Curves that show the grain-length orientation frequencies for feldspar porphyroclasts in WH31 with aspect ratios in the ranges 1.00–1.49, 1.50–1.99, 2.00–2.49 and 2.50–5.00. Discussion in text.

shear plane, but for grains of lower aspect ratio, the preferred orientation of grain-lengths will have rotated past the shear plane at lower shear strains (Benn & Allard 1989, p. 940, state that for an aspect ratio of 1.5 this takes place at a shear strain of 3.5). The gabbros analyzed by Benn and Allard demonstrate just such a relationship.

The SPO diagram (Fig. 2d) is not very asymmetrical, and the mean/median grain-length orientation and the maximum aspect ratio seem coincident. Re-examination of the original data shows that the actual orientation of the most elongate grain is 80° (counted in Fig. 2d as part of the interval 80–89°), again displaced relative to the position of the mean/median in the same way as in all the other parts of Fig. 2. Examination of the data for evidence that grains of different aspect ratios have rotated by different amounts, similar to that described by Benn & Allard (1989), did not reveal any convincing relationship. For grains with aspect ratios of 1.00–1.49, 1.50–1.99, 2.00–2.49, and >2.5, the frequency modes are essentially coincident (Fig. 7), and it remains unclear what was the actual orienting mechanism for the feldspar porphyroclasts.

CONCLUSIONS

The principal conclusions of this study are:

(1) Shape preferred orientations are commonly asymmetric, and the asymmetry is best displayed by a skewed curve derived by plotting the highest aspect ratio for various grain-length orientation categories. The median and mean grain-length orientations of the population as a whole should be marked on the skewed curve.

(2) Consistent relationships exist between the SPO and known senses of shear so that (a) the sense of rotation is given by rotating grains with length-orientations in the flatter or longer part of the skewed curve towards the orientation of the most elongate grain; (b) the same sense is also provided by rotating grains from the mean or median orientation towards the orientation of the most elongate grain.

(3) The asymmetries revealed by these plots are not usually obvious in thin section.

(4) The asymmetries occur in a wide range of materials, both as recrystallized mosaics and as discrete grains in metamorphic rocks, and in association with lattice preferred orientations that originated by a variety of mechanisms.

(5) The asymmetric SPO's are to be expected if *P* or *G*-type mechanisms were responsible for the preferred orientation. It is less clear what the relationship is to *M*-type mechanisms. The production of mica-fish, and concomitant shredding of mica, is similar geometrically to a *P*-type mechanism. The one example examined where rigid crystals developed a preferred orientation in ductile material is the least asymmetric of patterns, and provides little support for the orienting mechanism most commonly advocated.

Many of the relationships revealed by this work require further investigation. In particular, some of the angular relationships revealed in the plots of Fig. 2 are not fully understood, and one can expect new insights into the mechanisms of preferred orientation development from such investigations.

Acknowledgements—Kathryn Lewthwaite is thanked for the loan of specimen WH31. An earlier version of the paper benefited from discussions with Kay Cooper and Aaron Stallard, and the critical comments of Scott Johnson. I am grateful to the University of Canterbury for its support in various ways during the course of this work, and for funding under FRST Contract No. UOC313 which enabled specimen KP3 to be collected.

REFERENCES

Behrmann, J. H. & Platt, J. P. 1982. Sense of nappe emplacement from quartz *c*-axis fabrics; an example from the Betic Cordilleras (Spain). *Earth Planet. Sci. Lett.* **59**, 208–215.

Benn, K. & Allard, B. 1989. Preferred mineral orientations related to magmatic flow in ophiolite layered gabbros. *J. Petrol.* **30**, 925–946.

Berthé, D., Choukroune, P. & Jegouzo, P. 1979. Orthogneiss, mylonite and non-coaxial deformation of granites: the example of the South Armorican shear zone. *J. Struct. Geol.* **1**, 31–42.

Blanchard, J. P., Boyer, P. & Gagny, C. 1979. Un nouveau critère de sens de mise en place dans une caisse filonienne: le "pincement" des minéraux aux épontes. *Tectonophysics* **53**, 1–25.

Cox, S. F. & Etheridge, M. A. 1983. Crack-seal fibre growth mechanisms and their significance in the development of oriented layer silicate microstructures. *Tectonophysics* **92**, 147–170.

Cox, S. F. & Etheridge, M. A. 1989. Coupled grain-scale dilatancy and mass transfer during deformation at high fluid pressures: examples from Mount Lyell, Tasmania. *J. Struct. Geol.* **11**, 147–162.

Fernandez, A. 1987. Preferred orientation developed by rigid markers in two-dimensional simple shear strain: a theoretical and experimental study. *Tectonophysics* **136**, 151–158.

Fernandez, A., Feybesse, J. L. & Mezure, J. F. 1983. Theoretical and experimental study of fabrics developed by different shaped markers in two-dimensional simple shear. *Bull. Soc. geol. Fr.* **25**, 319–326.

Higgins, M. D. 1991. The origin of laminated and massive anorthosite, Sept Iles layered intrusion, Quebec, Canada. *Contrib. Mineral. Petrol.* **106**, 340–354.

Hippertt, J. F. 1994. Microstructures and *c*-axis fabrics indicative of quartz dissolution in sheared quartzites and phyllonites. *Tectonophysics* **229**, 141–163.

Ildefonse, B., Lardeaux, J. M. & Caron, J. M. 1990. The behaviour of shape preferred orientations in metamorphic rocks: amphiboles and

jadeites from the Monte Mucrone area (Sesia-Lanzo, Italian Western Alps). *J. Struct. Geol.* **12**, 1005–1011.

Ildefonse, B., Sokoutis, D. & Mancktelow, N. S. 1992. Mechanical interactions between rigid particles in a deforming ductile matrix. Analogue experiments in simple shear flow. *J. Struct. Geol.* **14**, 1253–1266.

Lister, G. S. & Williams, P. F. 1979. Fabric development in shear zones: theoretical controls and observed phenomena. *J. Struct. Geol.* **1**, 283–297.

March, A. 1932. Mathematische Theorie der Regelung nach der Korngestalt bei affiner Deformation. *Z. Kristal. ogr.* **81**, 285–297.

Miyake, A. 1993. Rotation of biotite porphyroblasts in pelitic schist from the Nukata area, central Japan. *J. Struct. Geol.* **15**, 1303–1313.

Oertel, G. 1985a. Reorientation due to grain shape. In: *Preferred Orientation in Deformed Metals and Rocks: An Introduction to Modern Texture Analysis* (edited by Wenk, H.-R.). Academic Press, Orlando, 259–265.

Oertel, G. 1985b. Phyllosilicate textures in slates. In: *Preferred Orientation in Deformed Metals and Rocks: An Introduction to Modern Texture Analysis* (edited by Wenk, H.-R.). Academic Press, Orlando, 431–440.

Passchier, C. W. & Simpson, C. 1986. Porphyroclast systems as kinematic indicators. *J. Struct. Geol.* **8**, 831–843.

Shelley, D. 1979. Plagioclase preferred orientation, Foreshore Group Metasediments, Bluff, New Zealand. *Tectonophysics* **58**, 279–290.

Shelley, D. 1981. The Pikikiruna nappe, northwest Nelson. *J. geol. geophys. New Zealand* **24**, 593–602.

Shelley, D. 1985. Determining paleo-flow directions from groundmass fabrics in the Lyttelton radial dykes, New Zealand. *J. Volcanol. & Geotherm. Res.* **25**, 69–79.

Shelley, D. 1989a. Plagioclase and quartz preferred orientations in a low-grade schist: the roles of primary growth and plastic deformations. *J. Struct. Geol.* **11**, 1029–1037.

Shelley, D. 1989b. *P*, *M* and *G* tectonites: a classification based on origin of mineral preferred orientations. *J. Struct. Geol.* **11**, 1039–1044.

Shelley, D. 1992. *Igneous and Metamorphic Rocks Under the Microscope*. Chapman & Hall, London.

Shelley, D. 1994. Spider texture and amphibole preferred orientations. *J. Struct. Geol.* **16**, 709–718.

Tullis, T. 1976. Experiments on the origin of slaty cleavage and schistosity. *Bull. geol. Soc. Am.* **87**, 745–753.

Vissers, R. L. M. 1993. Quartz *c*-axis fabrics in deformed conglomerates: some support for a skeletal approach to fabric analysis. *J. Struct. Geol.* **15**, 1055–1060.